Pak. j. life soc. Sci. (2024), 22(2): 723-748 E-ISSN: 2221-7630;P-ISSN: 1727-4915

Pakistan Journal of Life and Social Sciences

www.pjlss.edu.pk

https://doi.org/10.57239/PJLSS-2024-22.2.0053

RESEARCH ARTICLE

A Novel Deep Learning Approach for COVID-19 Case Identification: Enhanced CNN-KNN Hybrid Model with 5-Fold Cross-Validation

Dr. Nahid Kh Elfaki[1], Dr. Hasan Yahya Guzailan[2], Dr. Ahmed Abdo Abdullah Harwn[3], Mr. Abdulaziz Hassan Salem Alytimi[4], Dr. Samia Fathelrahman[5], Dr. Abdalla Mohamed Ahmed Osman[6], Dr. Yahya Hussein Ahmed Abdalla[7], Dr.Mohahmmed Hussein .M Hashlan[8], Dr.Ali Hadi Mesfer Alyami, [9], Dr.Nasser Mesfer Rashed Alabataheen[10] Dr. Abdulrahman Ahmed Harwn[11], Mr.Abdullah saeed omayr alrashdi[12], Dr. Shaza Dawood Rihan[13], *Dr. Sawsan Ahmed Awadallah Osman[14]

[1,6,7]Najran University; Saudi Arabia, College of Nursing Community & psychiatric H. Dept

[2,3,8,9,10] King Khalid Hospital, Najran, Radiology department

[11]The Jordaian Royal Medical Services, Jordon

[4,12]Najran Armed Forces Hospital, Radiology department

[13] Najran University; Saudi Arabia, Applied College -Computer department

[5,14] Najran University; Saudi Arabia, College of Applied Medical Sciences

ARTICLE INFO	ABSTRACT

Received: Apr 19, 2024

Accepted: Jul 29, 2024

Keywords

COVID-19
CNN model
KNN model
CNN-KNN hybrid model
Image resizing
Image classification
Image enhancing
Diagnosis

***Corresponding Author:**

Sawsanahmedawadallah@gmail.com

As RNA viruses, coronaviruses are responsible for the COVID-19 disease, which causes adverse effects on humans' lungs, heart, kidneys, and liver. Corona-viruses diagnosis relies on clinical examination besides traditional laboratory tests, which may not give quick and reliable results. Therefore, a hybrid machine learning hybrid CNN-KNN-based model with five-fold cross-validation as an ideal predictive model has been suggested and demonstrated. Nearly 2580 original CT scan images from 216 participants in a randomized controlled clinical trial were gathered and enhanced for the study. In order to extract features, a hybrid approach was used to integrate K-Nearest Neighbors (KNN) and Convolutional Neural Network (CNN) architecture. While categorizing CT scan cases, features were used from the model's fourth convolutional layer. Preprocessing techniques like contrast enhancement, median filtering, data augmentation, and scaling were applied to the photos. The dataset was split into five folds for testing using five-fold cross-validation and training to guarantee generalization and avoid overfitting. With four MAX-POOL levels, four CONVOLUTION layers, and two completely CONNECTED layers, the CNN model has twenty-three layers total. The k-nearest neighbor was utilized for feature categorization rather than soft-max to improve accuracy levels. The findings of the study revealed that the average score for accuracy was 98.39%, whereas the average score for precision was 98.56%, and for the recall, the average score was 97.28%, while FI scored 98.02% and 0.9859 as Area Under Curve (AUC) were achieved, respectively. This model can achieve an accuracy comparable to other state-of-the-art and custom CNN models. It was concluded that the currently suggested method for timely and accurate diagnosis of COVID-19 cases has been proven to be extremely effective.

INTRODUCTION

Coronavirus, a variant of the SARS family, became a global pandemic in the year 2019 and halted global activities and normal functioning of life for nearly three years. It has caused nearly 14.83 million people deaths and has caused global economic loss of trillions of dollars (Msemburi et al., 2023). The novel coronavirus disease (COVID-19) is an acute respiratory disorder and can cause mild to severe disorders in the lungs and other human vital organs (Ciotti et al., 2020). The virus outbreak has posed critical challenges for public health in various communities across the globe (Al Mutair et al., 2020; Harapan et al., 2020).

Although the vaccination and isolation procedure has given healthcare professionals and the public control over the spread of COVID-19, it still is a great global risk (Filip et al., 2022). Due to this, scientists, doctors, and policymakers must detect COVID-19 cases accurately. By April 23, 2020, there were around 750,000 reported recoveries, over 190,000 confirmed deaths, and 2.7 million confirmed cases (Wright, 2021). However, no data is provided to the public on examinations that might be neglecting infections. False negative test results might specifically complicate matters and increase anxiety (Kanji et al., 2021)

Corona-viruses diagnosis relies on clinical examination and traditional laboratory diagnostic techniques such as Real Time-Polymerase Chain Reaction (RT-PCR) (Teymouri et al., 2021). It is one of the most widely used laboratory methods for detecting the COVID-19 virus and is claimed to provide rapid and accurate results. Despite the numerous benefits of RT-PCR, it cannot detect whether the infection is newly acquired or has relapsed (Kanji et al., 2021). Understanding the history and pattern of infection relapse is crucial for understanding how viruses develop and spread. (Shyu et al., 2020).

Scientists have been working to develop a technique that can help obtain more detailed analysis results and can give more accurate and rapid results for COVID-19 diagnosis (Abdulkareem & Petersen, 2021). Multiple studies have shown that the use of AI technology in the medical field is increasing daily to combat diseases and their symptoms (Huang et al., 2021). In recent years, Machine Learning/Deep Learning techniques have been widely used to identify patterns in complex health data such as clinical imaging, genomics, bio-imaging, and phenotypic data (Khattab et al., 2023). As a subfield of Artificial intelligence (AI), Computer Vision (CV) has enjoyed recent success in solving various complex problems in the healthcare sector, including the COVID-19 problem (Ashtari, 2022; Tasnim & Qi, 2023).

Artificial intelligence and Machine learning are utilized in conjunction with radio imaging technologies such as computed tomography (CT), x-rays, and clinical blood sample data to improve the diagnosis and screening procedure of the identified patient (Alyasseri et al., 2022). Table 1, presented in the latter part of the study, shows a selection of data regarding the suggested diagnosis and screening methods for coronavirus illness (Benmalek et al., 2021). Moreover, a chest computed tomography (CT) scan is used to diagnose COVID-19. CT sometimes may need to give more timely, quick, and reliable results (Lee et al., 2020; Mohbey et al., 2022a).

In addition to computed tomography, another AI technique called Image classification or image labeling is found to be a crucial application of computer vision that involves the usage of Machine Learning (ML) and Deep Learning (DL) methods (Amyar et al., 2020; Krizhevsky et al., 2017).In order to improve image classification applications, a range of transfer learning techniques, including Mobile-Net, VGG-19, U-Net, Xception, and custom CNN models like Dark-COVID-Net, have been applied with accurate results (98.08%) (Ozturk et al., 2020; Wang et al., 2021). For example, Soares et al.'s work produced a dataset of CT scans from São Paulo hospitals with good predictive values and accuracy for diagnosing COVID-19. They show a positive predictive value of 99.2% with average accuracy of about 74.4% and 95.5% sensitivity, respectively (Soares et al., 2020)

A study by Silva et al demonstrated that a high-accuracy image retrieval technique, but as it depends on numerous parameters, it might only be appropriate to adapt that process in some circumstances. Due to multiple parameters being involved in the mentioned techniques, it is not easy to use them on memory-constrained machines (Silva et al., 2020). Although the method's intricacy may limit its practical implementation in some cases, it was created to attain high accuracy in image classification. The complexity of the method and the device's memory-linked restraint could be a disadvantage in some circumstances, even though its accuracy is excellent (Silva et al., 2020).

Henceforth it is essential to develop a quick, dependable, accessible, and affordable diagnostic method for COVID-19 and associated disorders in order to address the previously discussed problems (Vinod & Prabaharan, 2020). Therefore, an enhanced diagnostic system with superior performance, extreme accuracy, and rapid results is urgently needed. Multiple research has proposed employing an automated hybrid CNN-KNN technique with five-fold cross-validation to classify COVID-19 patients according to their CT scan results (Sejuti & Islam, 2023). The hybrid model method uses a K-nearest neighbor for classification and a multi-layered CNN for feature extraction (Chen et al., 2020; Kaur & Gandhi, 2022; Zouch et al., 2022).

A key objective of our study was to create the most accurate, rapid, and precise prediction model possible for identifying patients' CT scan results as COVID-19 positive or negative. The study adopted a hybrid CNN-KNN-based approach to create a prediction model. The suggested hybrid method combines machine learning (ML) with K-nearest neighbors (KNN) and deep learning (DL) using convolutional neural networks (CNN) (Choudhry et al., 2023). The study utilized two different datasets for the classification problem for combining CNN and KNN.

Convolutional neural networks are one of the widely employed deep learning techniques used for processing and recognizing images (Ardakani et al., 2020). The convolutional neural networks comprise multiple layers known as convolutional, pooling, and fully linked layers that make up these networks (Ardakani et al., 2020). CNNs are very efficient at spotting certain characteristics or observable features associated with certain diseases in CT scans (Ahsan et al., 2024). These characteristics are usually helpful in categorizing cases as positive (disease-bearing individuals) or negative (health-free individuals) (Hall et al., 2020). As a type of deep learning algorithm, Convolutional Neural Networks (CNNs) are the most popular and suitable for recognizing and processing images (Narin et al., 2021).

All three layers of convolutional neural networks play pivotal roles in image retrieval and classification (Staszewski et al., 2021). Convolutional layers are necessary to extract information such as edges, textures, and forms from the sample input images (Imani, 2021). The next step is image size adjusting, which usually occurs with the help of pooling layers; the output is sent through pooling layers, which retain the most important data (Alzubaidi et al., 2021). In the meantime, it samples the data, adjusts the feature maps, and reduces their spatial dimensions (Jain et al., 2021). In the end, fully connected layers, for classification or prediction or data obtained from images, pass the output of the pooling layers (Hafeez et al., 2023).

METHODOLOGY:

2.1 Study Participants:

Nearly 1300 CT scan images of COVID-19-infected patients had been collected from 52 males and 48 females of different ages, in addition to 1280 CT images collected from 56 males and 51 females who were COVID-19-free. These CT images were collected from 3 different public hospitals in Najran. CT scan images in the current dataset do not maintain a standard size, and the contrasts, too, were different. Table 1 below shows the data types that were obtained.

In its nature the mentioned study was a randomized controlled clinical trial. After checking the data, 20 CT images were noticed to be of bad lung field. Accordingly, they had been omitted.

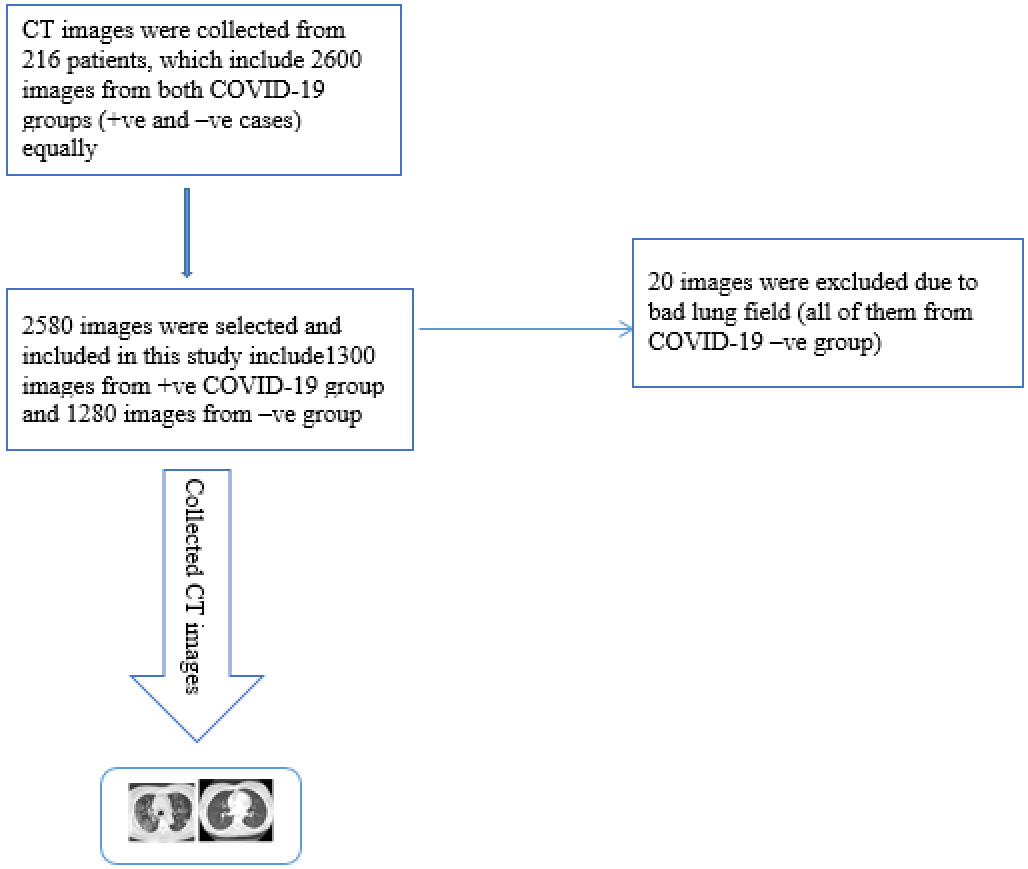

Figure1: Dataset selection flow-chart

All the collected CT images were ensured to be of COVID-19 positive patients and those who are suspected to be suffering from it, out of 1300 CT images which were collected from the suspected COVID-19 patients only 100 turned out to be true positive, while in the case of COVID-19 negative tests it was seen that nearly 116 were reported as false negative. Therefore, 2580 CT images were included in the dataset of the current study, as shown in Figure 1.

All the collected CT images were ensured to be of COVID-19 positive patients and those who are suspected to be suffering from it, out of 1300 CT images which were collected from the suspected COVID-19 patients only 100 turned out to be true positive, while in the case of COVID-19 negative tests it was seen that nearly 116 were reported as false negative. Therefore, 2580 CT images were included in the dataset of the current study, as shown in Figure 1.

Table 1: The included implementation dataset

Data type	Number of CT images	Number of cases
COVID-19 (+ve)	1300	100
COVID-19 free (-ve)	1280	116

Total	**2580**	**216**

2.1: Dataset and the system working process

The CT scan obtained from the images was detrimental in selecting the study model to verify whether the collected samples were positive or negative for the COVID-19 viral infection. Following the CT-scan results, the study shifted towards incorporating the hybrid CNN-KNN model. The model combines Convolutional Neural Networks (CNN), which excel in processing visual information such as images, with K-Nearest Neighbor (KNN), a machine learning technique that identifies patterns within datasets.

The working process for the CNN-KNN hybrid model takes place in five steps, as shown in Figure 2:

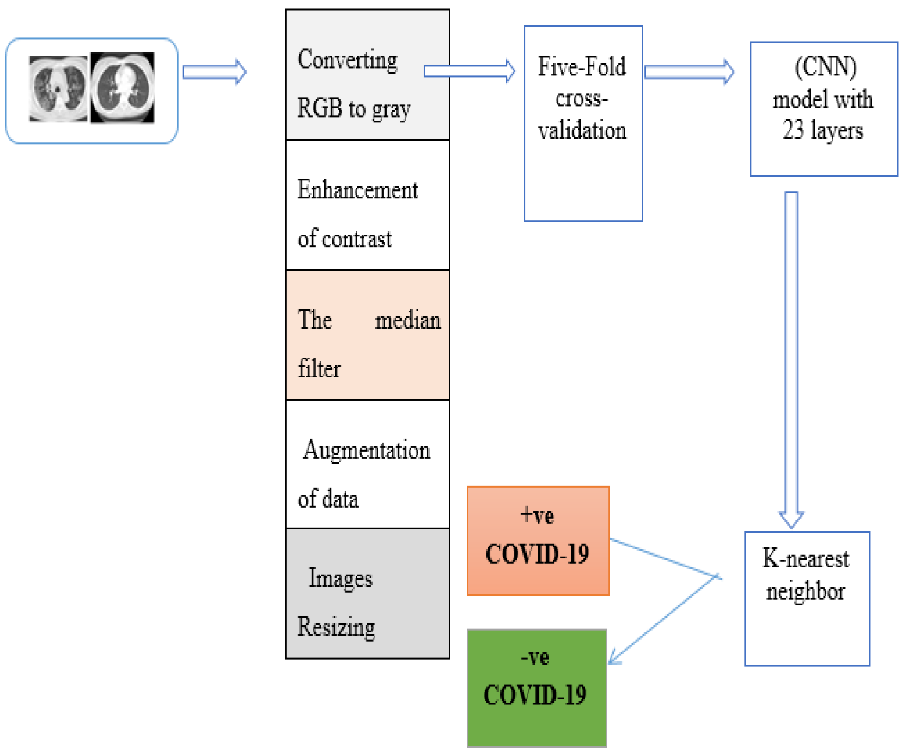

Classifier

Figure 2: An overview of the hybrid system's working process

2.2.1: The Image Uploading Phase (Step 1)

Step 1 of the CNN-KNN model, known as the image uploading phase, is highly crucial for the analysis of lung tissues as they are quite complicated. The preprocessing or image uploading step has five further steps AE), the first of which is the crucial step of converting RGB (Red, Green, and Blue) photos into Grayscale before finalizing the scaling of the images. The conversion is usually done because greyscale pictures contain fewer details than grey format images and thus are easy to handle computationally and analyze.

The CT-scan images of both the test and control groups were obtained from the raw data present in the data repository.

2.2.1.1 Stage A) Converting RGB images into grey format:

In the image processing technique, the Red-Green-Blue (RGB) color model is one of the most commonly employed models. However, the grey format is a far more preferred model, usually because it simplifies algorithms, is comparatively easy to analyze computationally, saves storage space, and grayscale conversion is important for multiple medical applications. The grey format is especially useful for complex calculations. The transformation of RGB into grey format, commonly calculated as Grayscale with the help of the following formula: Grayscale= (R + G + B)/3, simplifies the analysis procedure. The conversion cycle of original image from RGB theme to Gray theme has been shown in figure 3 mentioned below.

Figure (3): The first three steps in the preprocessing technique

COVID CASES	Original CT images	A: Gray CT images	B: Contrast enhanced CT images	C: Filtered median CT images
Non COVID-19 infected images				
COVID-19 infected images	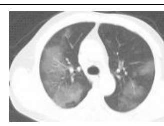		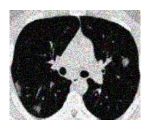	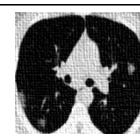

Figure 3 illustrates the first three steps in the preprocessing stage AC,) which include COVID-19 CT images (row number one) and non-COVID-19 CT images (row number two). Where the first column is for the original CT images (raw dataset). The preprocessing step starts with the gray CT images step in column A, followed by Contrast-enhanced CT images placed in column B, and the last column (C) for the filtered-median CT images.

In medical procedures such as diagnosis procedures, grayscale conversion is important, particularly when computer-aided diagnostic techniques are used with pictures from CT, X-ray, and ultrasound scans. In healthcare settings, the grey format is highly appreciated as it helps remove unnecessary coloring and detailing from the image, allowing precise assessments and treatment suggestions.

2.2.1.2 Stage B: Enhancement of contrast:

The next stage is enhancing the contrast of the images; this is done to correct the different contrast levels in the images. This is usually done to improve the visibility of the discreet structures present in the photographs, this facilitates in highly precise and more accurate analysis and interpretation of the images.

2.2.1.3 Stage C: Median filtration:

Once the contrast is adjusted, the next step is the application of median filtration. Median filtration is usually applied using a sliding window technique to reduce the noise in the photos. Using this method, the median value of the relevant window was used to replace the central pixel of a neighborhood with dimensions of N*N. The median filtration enhances the overall quality and smoothness of the image. Figure 4 demonstrates all the stapes included in the median filtration to enhance the quality of the images.

Figure 4: The Augmentation techniques used in median filtration

Categories	**(a)** Number of used original CT images	The used 4 Augmentation Techniques				The Number of Augmented Images
		(b) flipping	**(c)** reflection	**(d)** scaling	**(e)** shearing	
COVID-19 (+ve)	1300	210	218	205	205	838
COVID-19 free (-ve)	1280	205	205	205	205	820
Total	**2580**	**415**	**423**	**410**	**410**	**1658**

2.2.1.4 Stage D: Data Augmentation

The fourth preparation step is artificially expanding the dataset. Data expansion is usually done with the help of a data augmentation technique. Data augmentation is required by the Convolutional Neural Networks (CNN) training. (Hussain et al., 2017; Nguyen et al., 2021). The data augmentation technique helps in image training, preventing the model from overfitting. (Heidari et al., 2020). Before initiating the training, the model, the original images, or datasets underwent four different forms of data augmentation: flipping, reflecting, scaling, and shearing.

The study in focus employed 210 COVID-19 CT pictures and 205 COVID-free CT images to undergo vertical flips. Image X-shear was used for image shearing, resulting in distortion along the image axis. For this purpose, shearing angles were purposely set in the 0° to 30° range and rendered as important angles. The obtained results are mentioned in figure 4:

	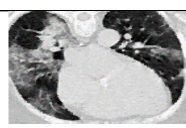	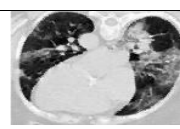	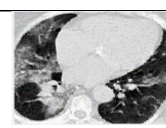	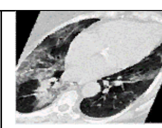
(a) COVID-19 (+ve) Original CT-scan images	(b)vertically flipped COVID-19 CT image	(c) 45° clockwise rotated CT scan	(d) scaled CT scan of a COVID-19 patient	(e) Sheared CT scan of a COVID-19 patient

Figure (4): Augmented CT images for COVID-19 +ve category (Original dataset)

The numerical data obtained from data augmentation is mentioned in Table 2. The original COVID-19 dataset consists of 2580 CT scans. Augmentation was adopted to increase the number of samples. After augmentation, the number of images increased to a total of 4225 images. Eight hundred thirtyeight images are related to the COVID-19 (+ve) category, while 820 are related to the COVID-19 free (-ve) category.

Table (2): Detailed augmented dataset images

Categories	**(a)**	The used 4 Augmentation Techniques				The Number of Augmented Images
	Number of used original CT images	**(b)** flipping	**(c)** reflection	**(d)** scaling	**(e)** shearing	
COVID-19 (+ve)	1300	210	218	205	205	838
COVID-19 free (-ve)	1280	205	205	205	205	820
Total	**2580**	**415**	**423**	**410**	**410**	**1658**

2.1.1.5 E: Images Resizing:

The next and final step of the image uploading phase is image resizing. The images obtained from the original dataset vary in size and are thus first resized to have the same pixels. In the case of our study, the dimensions of the input images were kept as 64*64 pixels, and the image pixel values at the edges were normalized from zero to one (0-1). In the current study, data augmentation was done using mirroring and data duplication with rotation. The figure 5 mentioned below pictorially represents the categorization of training and testing sets in each folding.

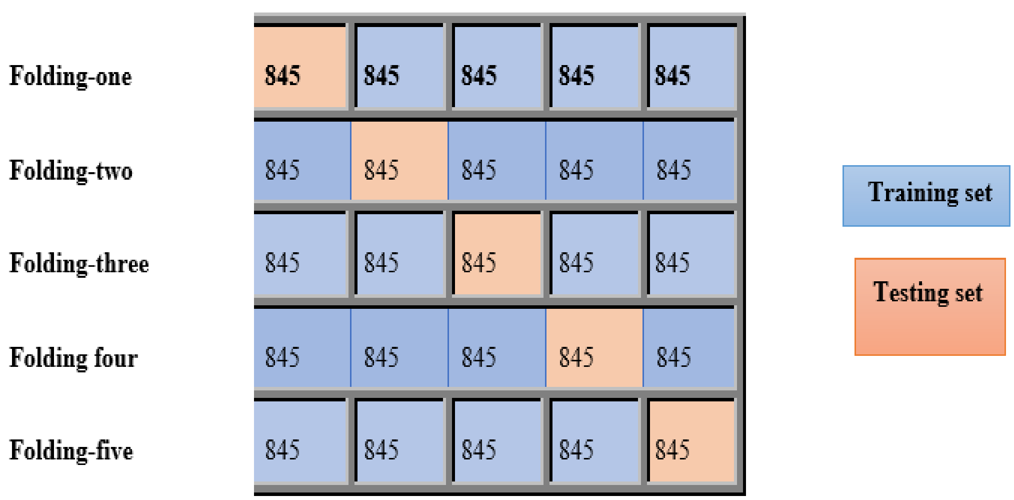

Figure 5. Splitting of Dataset with 5-fold cross-validation

During the preprocessing stage, the images' pixel values were converted to the range zero to one (0-1) by dividing them by 255, which is the maximum possible pixel value to be used for an image. CT images were also resized to 224*224 and used as inputs to the model. For testing the model, 20% of the dataset (845 CT images) was utilized, while 80% (3380 images) was used for training. During the training, 20% of the training CT images were used to validate the training performance. A computer cluster was used to conduct the entire experiment. The used computer's specifications were 11th Gen Intel core (TM) i7 Processors with 1TB SSD and 16 GB RAM.

2.2.2. Splitting dataset by Five-Fold cross-validation

The study uses part-to-part training and validation throughout the dataset rather than random splits. The original enlarged dataset, which started with 2580 photographs, increased to 4225 images after data augmentation and splitting them into five equal categories; each category had 845 images. Five trials of the folding technique were performed. Out of five segments, one segment (highlighted in pink as shown in Figure 5) was separated for validation in each fold, such as folding one, and the remaining segments were set aside for training. Subsequent folds systematically followed this pattern. Changing the training sets in each cycle was done to prevent overfitting, avoid bias, and foster the dataset.

2.1.3. Images Extraction Features

Now that the CT-scan images have been preprocessed, a distinct and new hybrid CNN-KNN model was created to identify COVID-19-positive samples from CT scan pictures. The proposed CNN model has twenty-three layers with four convolutional layers, including four max-pooling layers, one dropout layer, two fully connected layers, and a softmax layer for classification. As mentioned in the figure 6:

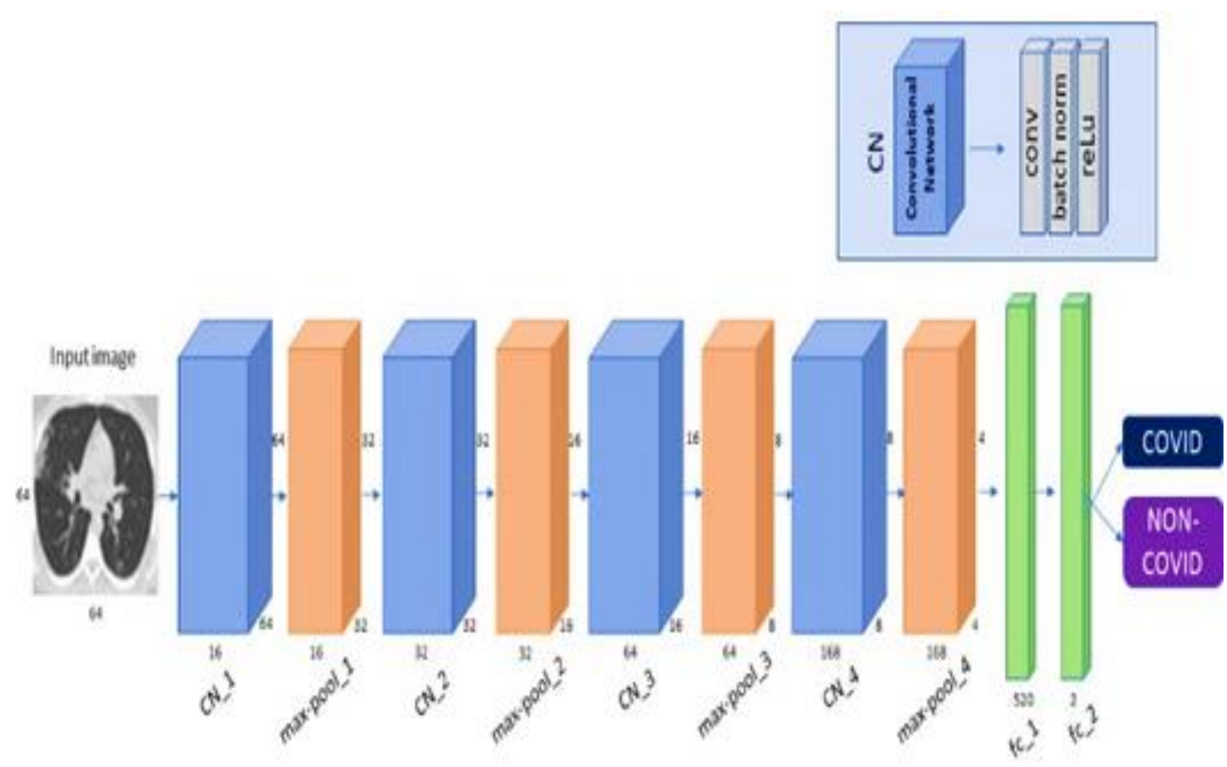

Figure 6: A proposed CNN architecture

The CNN network receives the enhanced image as input after its pixel has been shrunken to 64x64 pixels. The first convolutional layer processes input images and creates feature maps using a 5x5 kernel and 16 channels. This convolutional layer's output feature map is calculated using the following formula:

$$M_x^L = B_x^L + \sum_{y=1}^{N^{L-1}} F_{x,y}^L * M_y^{L-1}$$

Where MxL represents the output feature map, L is the layer, FxL, represents the filter, NL−1 stands for the number of filters, BxL is biased, and MyL−1 is the input map.

These feature maps store detailed information about features in the images. The 64*64 input image was convolved in the first convolutional layer with 16 filters. Following each convolution layer was a batch normalization layer and enhanced reLu activation.

A block denoted as CN comprises a single convolutional layer, a batch normalization layer, and a rectified linear unit (ReLU) layer, as depicted in Figure 4. The ReLU layers are employed as activation functions to enhance the non-linearity of the images. Following each convolutional block, a max-pooling layer with a kernel size 2x2 is utilized to summarize and downsample the generated feature maps. The following equation determines the calculation for convolving a single pixel from one layer to another:

$$N(x, y) = (i * w)[x, y] = \sum_m \sum_n i\ [m, n]\ w\ [x - m, y - n]$$

In the above-stated statistical formula, the N(x,y) is the output of the subsequent layer in convolutional neural networks; x and y represent the input picture and kernel size, respectively. The symbol '*' shows the convolution operation. The output of the first max-pool layer was used to pass 32 channels and a 5*5 kernel to the second convolution layer. The third and fourth convolutional 2-dimensional layers, with 64 and 168 channels, are given a 3*3 filter size. Table 3 displays each convolution layer's filter size and number of channels.

Table (3): Specifications of filter for convolutional layer:

Convolutional layers	Number of filters	Size of the filter
CONVO_1	16	5*5
CONVO_2	32	5*5
CONVO_3	64	3*3
CONVO_4	168	3*3

Five hundred twenty neurons formed two hidden layers comprising the fully connected layer, and two neurons comprise the flattening layer at the end of the max-pool layer. Two neurons were selected in the last fully connected layer for classifying COVID-19 patients (+ve cases) from non-COVID-19 patients (-ve individuals). Moreover, a dropout layer with a 0.5 dropout factor was applied in the center of two fully connected layers to regularize the model.

As a final point, the soft-max layer was used for class prediction because it can predict class probabilities. A CNN model has different layers of learnable parameters, as shown in Table (1).

Using the custom-designed CNN model, deep features are derived for identifying COVID-19. The proposed CNN model showed a simple representation of images by activating layers. However, the deeper the layer, the more complex the representation becomes. Interestingly, CT scan images of COVID-19 patients are classified according to the features highlighted in the activation.

Figure (7) displays the feature maps derived from each convolutional layer (from i-iv). The first (i) convolutional layer's low-level features weigh 16, While the feature maps represent mainly local features in terms of edges and shapes. The deeper fourth convolutional layer (iv) high-level feature map is also shown. Then, these features were fed into the K-nearest neighbor (KNN) classifier.

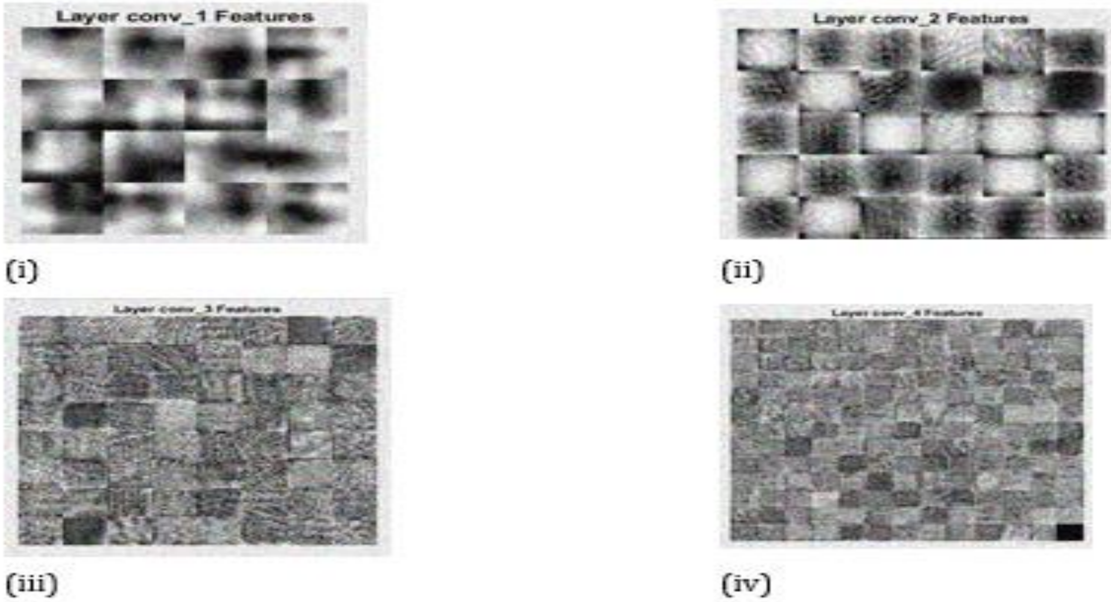

Figure (7): Feature map of convolutional layers

Figure (7) displays the feature map of convolutional layers as follow: Feature map of conv_1 layer (i), feature map of conv_2 layer (ii), while feature map of conv_3 (iii), and feature map of conv_4 is (iv).

2.1.4. CNN Model's Parameters

Learnable parameters were implemented using convolutional and fully connected layers (FC) to represent the weights obtained during CNN model training. The following formula is used to calculate the parameters (Pconv) for a convolutional layer:

$$\mathrm{P_{conv}} = \mathrm{F_h} * \mathrm{F_w} * \mathrm{F_{num}} * \mathrm{C_{in}} + \mathrm{F_{num}}$$

Fh represents filter height, while Fw expresses the filter width. Fnum denotes the number of filters, respectively. Cin represents the number of input channels for the corresponding layer. While the fully connected layer parameters (PFC) were represented as:

$$P_{FC} = A_{(prev)} * N_{(unit)} + N_{(unit)}$$

The fully connected layers (FC) and convolutional layers' parameters are computed in the suggested model. The help of learnable and non-learnable parameters represents the weights the CNN model learned during training. A convolutional layer's parameter is computed using the formula where N_(unit) is the number of units, or neurons, in the current FC layer, and A_(prev) is the dimension of the activation of the prior layer. In order to determine the parameters for the batch-normalization layer, the channel count of the preceding convolutional layer is multiplied by four. However, there are no learnable parameters in the max-pool layer. The present model has 1,530,242 parameters with 1,529,122 learnable parameters and 1,120 non-learnable parameters, as shown in Table (4).

Table (4): The Total Number of Parameters.

Layers	Activation Shape	Learnable Parameters
conv_1	64x64x16	416
batchnorm_1	64x64x16	64

relu_1	64x64x16	0
maxpool_1	32x32x16	0
conv_2	32x32x32	12832
batchnorm_2	32x32x32	128
relu_2	32x32x32	0
maxpool_2	16x16x32	0
conv_3	16x16x64	18496
batchnorm_3	16x16x64	256
relu_3	16x16x64	0
maxpool_3	8 x8 x 64	0
conv_4	8 x8 x168	96936
batchnorm_4	8 x8 x168	672
relu_4	8 x8 x168	0
maxpool_4	4 x4 x168	0
fc_1	1 x 1 x520	1398280
fc_2	1 x 1 x 2	1042
Total		**1529122**

2.1.4.1- Soft-max function:

After completely linked layers, CNN models use the soft-max function, also called the normalized exponential function or soft-argmax. The output values are normalized into a probability distribution using this activation function. The following is the mathematical definition of the soft-max activation function:

$$\mathrm{Softmax}(a_i) = \frac{e^{a_i}}{\sum_{j=1}^{n} a_j}$$

The soft-max activation function was used to convert the output into probability measures. Where (ai) represents the set of (n) number of variables. The soft-max activation was utilized to convert the output into a probability measure. Interestingly, CNN's training process is driven by this activation function, using a cross-entropy loss function by the following equation:

$$L_f = -\sum_i x^i \log x_i^{\prime}$$

Where Lf defines the cross-entropy loss function, while the real and predicted output values were symbolized by x and χ' respectively, the loss will be lower in situations where actual and predicted values are closer. An important part of training and calculating the gradient is the CE-loss function, which measures how close the actual and predicted values are. If a prediction is incorrect, the mean square error is heavily penalized. Accordingly, Mean Squared Error is not recommended for probabilistic output.

ii- K-nearest neighbour

K-Nearest Neighbors (K-NN) is a cornerstone machine learning (ML) classification approach, distinguished by its supervised and non-parametric features. The geometric technique is used in K-NN classifiers to calculate the distance between two points by taking the square root of the total squared differences between features. The following formula is used to express this distance calculation:

$$R = \sqrt{\sum_{i=1}^{N} (x_i - y_i)^2}$$

In this case, (R) stands for the Euclidian distance between two points, while xi-yi represents the two points in the (X, Y) plane), and (i) = 1,2,3,……., whereas (N) denotes the number of data points. In order to apply KNN accurately, an appropriate value of (K) must be selected, as its accuracy depends on this value respectively (Le, 2018). Therefore, in the current proposed work, the number of nearest neighbors (K) was set to three (3). Accordingly, the distance between the features specified for training and testing samples was calculated in the KNN (Zhang & Li, 2021). A majority voting class of the training features used in the KNN algorithm is centered around Euclidian distances. The following equation represents the majority rule algorithm:

$$M.R = \sum_{L(a_i,b_i)\epsilon D_r}^{argmax} I\,(L = b_i)$$

In which, (M.R) stands for majority voting rule, the classes are labeled with (L), while (I) denoted the function that adopted binary values to represent whether true or false. And (b_i) represents the i^{th} nearest neighbor of class label respectively. Compared with CNN, the use of KNN classifier is considered simple, no training time is required, and beside that it's more effective.

The fourth convolutional layer's high-level characteristics are collected and used as input in the K-Nearest Neighbour (KNN) classifier. The KNN classifier method maintains key qualities in order to categorise CT scan pictures of patients with and without COVID-19 based on their similarity to nearby or well-known features. The KNN algorithm uses features taken from the test images for classification or prediction. A total of 3,380 CT scan pictures were used in this study—845 for testing and 3,380 for training. The figure shows the scatter plots that show the test and training properties of the KNN classifier for the samples.

Figure (8): Scattering plots of KNN for (a) 1st fold (b) 2nd fold (c) 3rd fold (d) 4th fold (e) 5th fold.

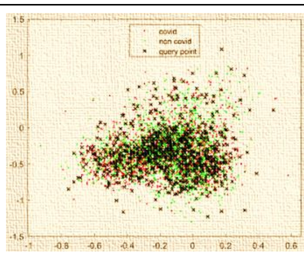	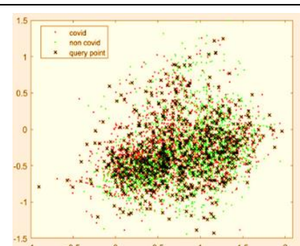
First fold (i)	Second Fold (ii)

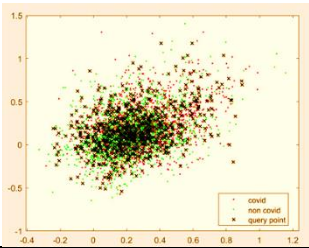

Third Fold (iii)

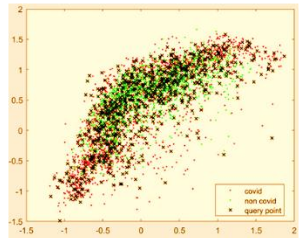

Fourth Fold (iv)

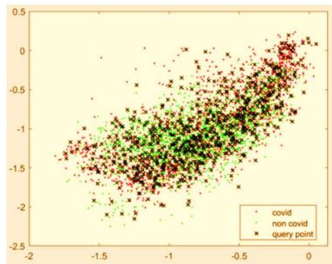

Fifth Fold (v)

As presented in figure (8), the augmented dataset had been divided into five folds, that resulting in five scatter plots. Each fold has different training and testing images resulting in the formation of five sets of training and testing features. As shown in this figure, the training features for COVID-19 are marked as red dots, while the green dots stand for the non-COVID-19 features. Additionally, the testing features are represented by a query points (x) in the scatter plot.

RESULTS

3.1) A) Hyper-parameters Training

Adaptive Moment Estimation (Adam) optimizer was utilized with the learning rate of 0.001 to train the CNN model. Due to its better performance specially in augmented dataset, Adam was chosen over the Stochastic Gradient Descent with Momentum (SGDM) optimizer. Since Adam combines two distinct optimizers (i. e. RMSprop and AdaGrad) (Kinga & Adam, 2015). Table 5 highlights a list of the training hyper-parameters.

Table (5): Training Hyper-parameters

Hyper Parameters	Specifications
Optimizer	Adam
Validation Frequency	10
Initial Learning Rate	0.001
Batch Size	163
Epochs	10
Learn Rate Drop Factor	0.2
Iteration /epoch	25

The training images (dataset) were adapted to the CNN model using batches of 163. Validation occurred ten times per training cycle. Therefore, the proposed model runs twenty-five iterations per epoch and completes ten epochs. After every fifth epoch, a drop factor of 0.2 was applied to decrease the learning rate. Figure (9) depicts the progression of five-fold cross-validation during the training process:

Figure (9): Training and validation accuracy of CNN model for five folds F-validation.

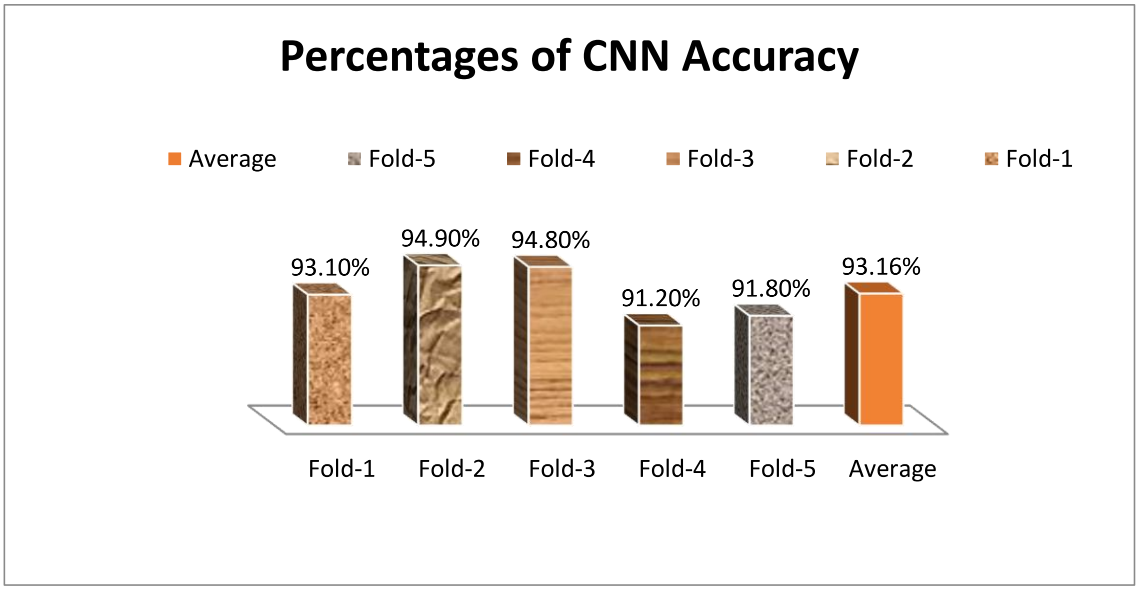

The epoch for training of CNN-KNN hybird model was set at 10 epoches. The 10 epoch value was decided because the graph become saturated after 10 epoch and the error rate remain unaffected. It was also seen that the The CNN model was able to achieved the highest accuracy for five folds after 10 epochs as displayed in Figure (9).

The acquired validation accuracy levels from each five-fold cross-validation as presented in table (6) were 93.10%, 94.90%, 94.80%, 91.20%, and 91.80%. While the average validation accuracy was 93.16% respectively.

Table (6): CNN and CNN-KNN Accuracy percentages

Number of the fold	Percentage of CNN accuracy	Percentage of CNN-KNN accuracy
Fold-1	93.10%	98.20%
Fold-2	94.90%	98.40%
Fold-3	94.80%	98.90%
Fold-4	91.20%	97.90%
Fold-5	91.80%	98.10%
Average	**93.16%**	**98.30%**

3.2) B. A better performance with KNN

Using KNN after CNN is a way to reduce the bias, as KNN regularizes the CNN result by using the extracted features. Since CNN uses the soft-max activation function, the result becomes biased towards training, therefore, using KNN after CNN can reduce the bias respectively.

3.3) Performance Assessment

To estimate the performance of the proposed CNN and CNN-KNN hybrid model, the following equations must be used to differentiate the actual and predicted classes from confusion matrices (Table 12 and 13). While referring to mentioned results it is necessary to understand about the terms ‘true positive’ refers to the state when a COVID-19 patient is correctly diagnosed with COVID-19. On the other hand, an incorrect diagnosis of COVID-19 is referred to as a 'false positive', or someone who is not COVID-19 is recognised as a COVID-19 patient.

Due to the higher true positive rate, the performance evaluation parameters precision and recall are also higher. This increases the accuracy of the proposed model as well. The confusion matrices are derived from the KNN classifier are presented in tables (7-11) as follow:

Table (7): CNN-KNN confusion matrix (fold-1)

Confusion Matrix		Predicted	
		COVID-19 (+ve)	Non-COVID-19 (-ve)
Actual	COVID-19 (+ve)	409	14
	Non-COVID-19 (-ve)	4	393

The table 7 focuses on the confusion matrix given for fold 1 and suggests a promising CNN-KNN model for COVID-19 diagnosis. It shows a high number of correct classifications, with 409 true positives and 393 true negatives, which indicates good overall performance on "fold-1" of the cross-validation process.

Table (8): CNN-KNN confusion matrix (fold-2)

Confusion Matrix		Predicted	
		COVID-19 (+ve)	Non-COVID-19 (-ve)
Actual	COVID-19 (+ve)	409	16
	Non-COVID-19 (-ve)	3	392

The table 8 shows a confusion matrix, which provides information about how well the CNN-KNN hybrid model classified COVID-19 cases. Even though the model has produced a high number of accurate classifications 409 true positives and 392 true negatives. The model gave a total of 16 cases as false positives and 3 cases as false negative.

Table (9): CNN-KNN confusion matrix (fold-3)

Confusion Matrix		Predicted	
		COVID-19 (+ve)	Non-COVID-19 (-ve)
Actual	COVID-19 (+ve)	407	12
	Non-COVID-19 (-ve)	5	396

The table 9 shows the CNN-KNN model's COVID-19 classification performance by the help of confusion matrix (fold-3). It gave 396 cases as true negative for COVID-19 and 407 as true positive for COVID-19. However, the fold 3 also reports 5 false positive cases and nearly 12 false positive cases.

Table (10): CNN-KNN confusion matrix (fold-4)

Confusion Matrix		Predicted	
		COVID-19 (+ve)	Non-COVID-19(-ve)
Actual	COVID-19 (+ve)	411	14
	Non-COVID-19 (-ve)	1	394

The table 10 shows that model gave a total of 411 cases of COVID-19 as True Positives and 394 cases of non-COVID-19 as True Negatives were accurately identified by the model. The forth fold of the model however, failed to diagnose one case of COVID-19 as False Negatives and misclassify 14 non-COVID-19 cases as COVID-19 False Positives.

Table (11): CNN-KNN confusion matrix (fold-5)

Confusion Matrix	Predicted	
	COVID-19 (+ve)	Non-COVID-19 (-ve)

Actual	COVID-19 (+ve)	410	13
	Non-COVID-19(-ve)	2	395

Table 11 shows the confusion matrix for the fold 5. The fold 5 gave total of 410 as true positive and 395 as true negative cases. As far as false positive and false negative is concerned a total of 13 cases were reported as false positive and 2 cases as false negative.

All the five folds (1-5) gave the true positive rates of COVID-19 images as 409, 409, 407, 411, and 410, while the actual number of testing COVID-19 CT scans was 412 respectively. Moreover, the true positive rates of the normal or negative COVID-19 CT scans for the all five folds were 393, 392, 396, 394, 395, whereas, the actual number of testing the normal (-ve COVID-19) was 408 respectively.

The graphical analysis for COVID-19 positive cases gave the average precision, recall and F1 scores were 98.56%, 97.28% and 98.02%, respectively. Conversely, for COVID-19-negative persons, the average precision, recall and F1 score were 96.94%, 98.48% and 98.14%, respectively as mentioned in the figure 10.

Figure (10): CNN Model Performance Evaluation Parameters

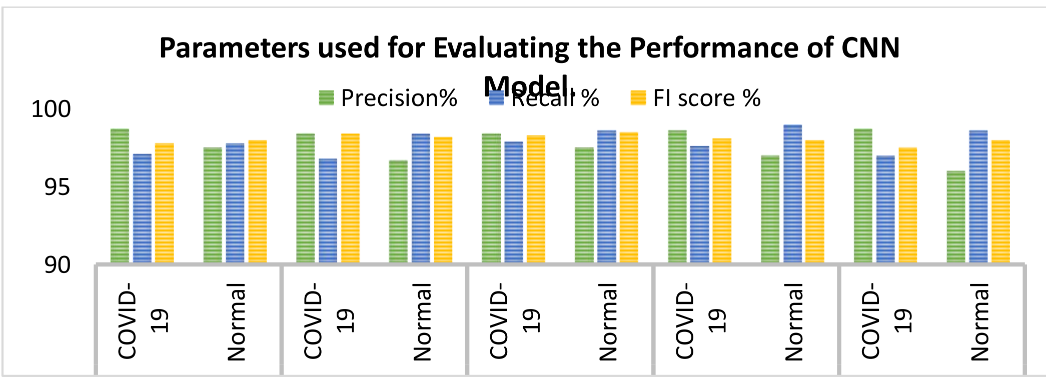

The figure 11 depicts that the precession value obtained through the CNN-KNN hybrid model is nearly about 99.5% which is the highest obtain precession value for both the CNN and KNN model. The high precision value indicates that the model rarely gives the false positive errors. The figure also shows that the re-call percentage deviates from 95% to 97% which indicates the model has very low frequency of producing false positive results. Whereas the FI score ranges somewhere between 96 to 99% which indicates that there is balance between the occurrence of both false positive and false negative results. As compared to results obtained from non-hybird models the values from hybrid model are quite high.

Figure (11): CNN-KNN Model Performance Evaluation Parameters

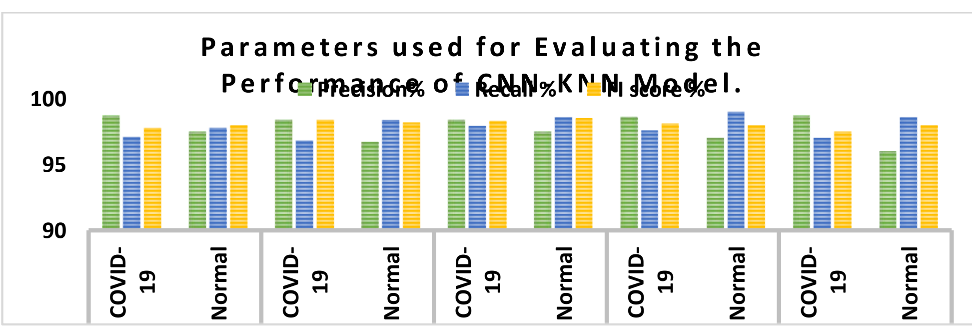

Comparative analysis and discussion

Artificial intelligence (AI) plays a pivotal role as in the field of medical imaging and research, it has led to major breakthroughs in both diagnostic and therapeutic aspects of medical field (Ahmad et al., 2021). The shear importance of AI is contributed to its ability to quickly and efficiently process large volumes of medical pictures providing timely identification and detection of disease (Manickam et al., 2022). AI's current application in radiation oncology and radiology demonstrates how it has improved medical imaging procedures (Parkinson et al., 2021).

The complexity and dynamic nature of AI applications in medical picture processing has revolutionized the application of image processing such as diagnostics (Mijwil et al., 2023). Improvements driven by artificial intelligence (AI) have greatly enhanced many picture applications in healthcare and other fields (Panayides et al., 2020). Bohr and Memarzadeh are confident that AI-powered deep learning models may be able to help doctors diagnose complicated medical conditions more quickly by assisting them in reading CT scans (Date et al., 2024). There are a number of studies that uses our selected dataset to attempt to identify

Multiple studies have shown the employing digital soft wares and medical imaging techniques such as usage of machine learning, deep learning and AI logarithms has given significant results (Ahmad et al., 2020). In order to detect COVID-19, medical imaging is essential as it provide insight of the infection progression at the cellular levels, it is especially essential when multiple different artificial intelligence (AI) methods are being involved in the diagnostics measures (Crunfli et al., 2022).

Recent studies have indicated that the use of deep learning and machine learning techniques is trending in the analysis of medical pictures, like computed tomography (CT) scans and chest X-rays (CXR), in order to identify COVID-19 patients (Shyni & Chitra, 2022). Research has demonstrated the efficacy of employing multiple machine learning (ML) techniques, such as supervised learning, deep learning, active learning, transfer learning, and evolutionary learning mechanisms, in the identification of COVID-19 from medical images (Bhattacharya et al., 2021). These methods use artificial intelligence (AI) algorithms to categories photos as COVID-19 positive or negative; deep learning and transfer learning are two of the most widely used strategies (Albahri et al., 2020).

Recent studies have shown that mechine learning technique such as Convolutional neural networks (CNNs), have shown excellent accuracy in identifying the presences of virus from X-ray and CT images (Rasheed et al., 2021). CNNs technique have been widely used in COVID-19 diagnosis studies. Numerous researches have been conducted to compare the various CNN models and their findings have emphasized how crucial model complexity and dataset quantity are to getting reliable findings (Alzubaidi et al., 2021). For example, in recent conducted researches new machine learning and AI models such as VGG16 have demonstrated better accuracy performance when trained on larger datasets compared to earlier research (Sitaula & Hossain, 2021).

Another well-known machine learning method that has been stealing spotlight in COVID-19 diagnosis is the K-Nearest Neighbours (KNN) algorithm. KNN approach has also been incorporated in our study (Darwaish, 2022). The unique feature of KNN that distinguishes it from deep learning techniques, is that KNN uses the average euclidean distance between samples to identify the closest neighbours rather than requiring complicated feature extraction (Kumar et al., 2024). This feature of KNN make it comparatively easy to study and use. Although KNN works well for small class prediction, its non-parametric character makes it difficult to incorporate with deep learning models (Zhang et al., 2023).

Multiple studies have suggested that the efficacy of machine learning and deep learning techniques can be used in a hybrid CNN-KNN model to identify COVID-19 from CT scans (Sejuti & Islam, 2023). In this model, a K-Nearest Neighbours (KNN) classifier is combined with a Convolutional Neural

Network (CNN) as a feature extractor. The average accuracy rate is reported to be somewhere around 98.26% after five rounds of cross-validation (Kumar et al., 2023). Our study has also shown that the outcomes of hybrid approach are more efficient and better as compared to techniques adapted separately. As per figure 10 and 11 it is quite evident that the efficacy of CNN model is somewhere around 95% while the efficacy of CNN-KNN hybrid model gave the efficacy of 98.5%.

COVID-19 positive individuals; a selection of these studies is provided in Table 12.

Table 12. Parameters used for Performance Evaluation of CNN-KNN with existing methods with the same dataset.

Studies	method	Number of Images		Accuracy
		COVID-19 (+ve)	COVID-19 (-ve)	
Xin He (36)	MNas3DNet4 (CNNs)	1515	965	88.63%
Mishra (37)	DEnseNet121(Deep CNN)	360	397	88%
Gaur (38)	Empirical wavelet transformation (EWT)	1252	1230	85.5%
Do, Vu L.(39)	F-EDNC	1252	1229	97.55%
Anwar & Zakir(40)	EfficientNet	351	396	90%
Mohamed et al(41)	Weakly-Supervised Network	3520	19,353	77%
Our proposed model	CNN-KNN-5	1300	1280	98.30%

Although previously suggested models are quiet efficient but their certain characterstics made them inappropriate to be used for small devices. However, the suggested hybrid model demonstrated unique performance measures and is more appropriate to be used by mobile devices, the obtained results of our model quite varied from the reported studies. Many research has investigated the use of similar datasets to find positive instances in the field of Covid-19 detection. Anwar & Zakir, Do & Vu, Gaur et al., He et al., Mishra et al., and Mohammed et al have all produced noteworthy research that has provided insightful information. Although the results of these investigations differ, our suggested model shows distinct performance outcomes in comparison to previous research outcomes. The significance of ongoing research and innovation in this subject is shown by the range of findings, which also emphasizes the complexity and dynamic nature of AI applications in medical picture processing.

Similarly, Mohbey et al conducted an extensive experiment by using 3 deep learning methods, which were VGG19, Xception Net, and CNN. Their results indicate that the opted models have achieved accuracy rates above 95% and Area Under Curve (AUC) up to 95% too (Mohbey et al., 2022b). Furthermore, it was seen that the effeciency of AI techniques depends on the availability of datasets with a wide range of quality, especially those appropriate for deep learning.

In the realm of medical applications, a significant hurdle for the advancement of deep learning techniques lies in acquiring extensive and dependable datasets. This challenge, as underscored by a research conducted in 2018 that emphasizes the critical importance of large and reliable datasets in the development of deep learning methods for medical purposes. The lack of datasets becomes a great obstacle that researchers and practitioners must address to increase the efficacy and applicability of deep learning in healthcare settings. (Xiao et al., 2018).

Advantages Of Study:

The CNN-KNN hybrid model has the ability to achieve significantly higher accuracy by utilizing the advantages of K-nearest neighbours (KNN) for fine-tuned images that plays great role in decision-making and convolutional neural networks (CNN) for efficient feature extraction (Sejuti & Islam, 2023). An additional layer of strength is added by the visual interpretability of CT scans, which gives doctors a concrete picture of the model's decision-making process and may boost their trust in the results of diagnosis. Additionally, by combining deep learning with more conventional machine learning methods, the integration of many methodologies gives the model a more complete and perhaps reliable tool for accurate COVID-19 detection (Alqudah et al., 2020).

Limitations Of The Study:

Although the hybird CNN-KNN model has a long list of its advantages as compared to traditional models it still has its own short comings. The quality and diversity of the CT scan dataset are critical to the model's success, so biassed or limited data can provide problems. Hybrid models' high computational complexity may also provide real-world difficulties, especially in healthcare settings where computational resources are limited (Alimadadi et al., 2020). Interpretability may be a problem since it may be difficult for physicians to comprehend the complex inner workings of the hybrid CNN-KNN model, which could prevent its broad adoption. It is important to properly handle ethical issues such as patient privacy, informed permission, and potential biases in training data (Varalakshmi et al., 2021).

Future Implications Of The Study:

There is amazing potential implications which arises from using a hybrid CNN-KNN model for COVID-19 identification via CT images. The hybrid method uses K-nearest neighbours (KNN) for more sophisticated decision-making and deep learning (CNN) for feature extraction and pattern identification. The hybrid method may eventually lead to more precise and trustworthy diagnostic instruments. By using explainability methodologies, AI-driven diagnoses may gain greater credibility and be accepted by the medical community. Further study in this area could result in personalised medicine strategies that adjust treatment plans according to unique patient profiles found by sophisticated AI analysis of medical imaging.

CONCLUSION:

This study mainly focuses on the usefulness of combining CNN architecture with KNN for classifying CT images as COVID-19 positive or negative. Moreover, K-fold cross-validation was used to improve the CT scan dataset's generalizability to obtain more precise and specific results. This methodology is strong in its foundation since it uses two different algorithms, which is one of its strengths. The results of our suggested method highlight the advantages and potential of using deep learning methods for quick and automated COVID-19 diagnosis.

Acknowledgments

The authors would like to express their gratefully appreciation to the Ministry of Education and the Deanship of Scientific Research at Najran University- Saudi Arabia for their financial and technical support under code number (NU/NRP/SEHRC/12/17).

Conflicts of Interest:

All authors declare that they don't have any potential conflicts to be declared.

Author Contributions

Conceptualization, N.E. and M.A.; Data collection and curation, S.A. and S.F.; formal analysis, A.O.; Y.A.; investigation, H.G. and A.H.; methodology, Sh.R., and A.A.; validation and visualization, S.A. and A.I.; writing original draft.; review and editing, M.A. All authors have read the final version and agreed to be published.

REFERENCES

Abdulkareem, M., & Petersen, S. E. (2021). The promise of AI in detection, diagnosis, and epidemiology for combating COVID-19: beyond the hype. Frontiers in Artificial Intelligence, 4, 652669.

Ahmad, H. M., Khan, M. J., Yousaf, A., Ghuffar, S., & Khurshid, K. (2020). Deep learning: a breakthrough in medical imaging. Current Medical Imaging, 16(8), 946-956.

Ahmad, Z., Rahim, S., Zubair, M., & Abdul-Ghafar, J. (2021). Artificial intelligence (AI) in medicine, current applications and future role with special emphasis on its potential and promise in pathology: present and future impact, obstacles including costs and acceptance among pathologists, practical and philosophical considerations. A comprehensive review. Diagnostic pathology, 16, 1-16.

Ahsan, M., Khan, A., Khan, K. R., Sinha, B. B., & Sharma, A. (2024). Advancements in medical diagnosis and treatment through machine learning: A review. Expert systems, 41(3), e13499.

Albahri, O., Zaidan, A., Albahri, A., Zaidan, B., Abdulkareem, K. H., Al-Qaysi, Z., Alamoodi, A., Aleesa, A., Chyad, M., & Alesa, R. (2020). Systematic review of artificial intelligence techniques in the detection and classification of COVID-19 medical images in terms of evaluation and benchmarking: Taxonomy analysis, challenges, future solutions and methodological aspects. Journal of infection and public health, 13(10), 1381-1396.

Al Mutair, A., Alhumaid, S., Alhuqbani, W. N., Zaidi, A. R. Z., Alkoraisi, S., Al-Subaie, M. F., AlHindi, A. M., Abogosh, A. K., Alrasheed, A. K., & Alsharafi, A. A. (2020). Clinical, epidemiological, and laboratory characteristics of mild-to-moderate COVID-19 patients in Saudi Arabia: an observational cohort study. European Journal of Medical Research, 25(1), 1–8.

Alshazly, H., Linse, C., Barth, E., & Martinetz, T. (2021). Explainable COVID-19 detection using chest CT scans and deep learning. Sensors, 21(2), 455.

Alyasseri, Z. A. A., Al-Betar, M. A., Doush, I. A., Awadallah, M. A., Abasi, A. K., Makhadmeh, S. N., Alomari, O. A., Abdulkareem, K. H., Adam, A., & Damasevicius, R. (2022). Review on COVID-19 diagnosis models based on machine learning and deep learning approaches. Expert systems, 39(3), e12759.

Alzubaidi, L., Zhang, J., Humaidi, A. J., Al-Dujaili, A., Duan, Y., Al-Shamma, O., Santamaría, J., Fadhel, M. A., Al-Amidie, M., & Farhan, L. (2021). Review of deep learning: Concepts, CNN architectures, challenges, applications, future directions. Journal of big Data, 8, 1-74.

Amyar, A., Modzelewski, R., Li, H., & Ruan, S. (2020). Multi-task deep learning based CT imaging analysis for COVID-19 pneumonia: Classification and segmentation. Computers in Biology and Medicine, 126, 104037.

Anwar, T., & Zakir, S. (2020). Deep learning based diagnosis of COVID-19 using chest CT-scan images. 2020 IEEE 23rd International Multitopic Conference (INMIC), 1–5.

Ardakani, A. A., Kanafi, A. R., Acharya, U. R., Khadem, N., & Mohammadi, A. (2020). Application of deep learning technique to manage COVID-19 in routine clinical practice using CT images: Results of 10 convolutional neural networks. Computers in Biology and Medicine, 121, 103795.

Ashtari, H. (2022). What is Computer Vision? meaning examples and applications in 2022. Computer Vision Meaning, Examples, Applications.

Benmalek, E., Elmhamdi, J., & Jilbab, A. (2021). Comparing CT scan and chest X-ray imaging for COVID-19 diagnosis. Biomedical Engineering Advances, 1, 100003.

Bhattacharya, S., Maddikunta, P. K. R., Pham, Q.-V., Gadekallu, T. R., Chowdhary, C. L., Alazab, M., & Piran, M. J. (2021). Deep learning and medical image processing for coronavirus (COVID-19) pandemic: A survey. Sustainable cities and society, 65, 102589.

Bohr, A., & Memarzadeh, K. (2020). The rise of artificial intelligence in healthcare applications. In Artificial Intelligence in healthcare (pp. 25–60). Elsevier.

Chen, J., Wu, L., Zhang, J., Zhang, L., Gong, D., Zhao, Y., Chen, Q., Huang, S., Yang, M., & Yang, X. (2020). Deep learning-based model for detecting 2019 novel coronavirus pneumonia on high-resolution computed tomography. Scientific Reports, 10(1), 19196.

Choudhry, I. A., Qureshi, A. N., Aurangzeb, K., Iqbal, S., & Alhussein, M. (2023). Hybrid Diagnostic Model for Improved COVID-19 Detection in Lung Radiographs Using Deep and Traditional Features. Biomimetics, 8(5), 406.

Ciotti, M., Ciccozzi, M., Terrinoni, A., Jiang, W.-C., Wang, C.-B., & Bernardini, S. (2020). The COVID-19 pandemic. Critical reviews in clinical laboratory sciences, 57(6), 365-388.

Crunfli, F., Carregari, V. C., Veras, F. P., Silva, L. S., Nogueira, M. H., Antunes, A. S. L. M., Vendramini, P. H., Valença, A. G. F., Brandão-Teles, C., & Zuccoli, G. d. S. (2022). Morphological, cellular, and molecular basis of brain infection in COVID-19 patients. Proceedings of the National Academy of Sciences, 119(35), e2200960119.

Darwaish, A. (2022). Adversary-aware machine learning models for malware detection systems Université Paris Cité].

Date, P., Pimprale, V., & Mandke, S. (2024). Original Research Article Explorative study on potential of machine learning and artificial intelligence for improved healthcare diagnosis and treatment. Journal of Autonomous Intelligence, 7(3).

Dong, D., Tang, Z., Wang, S., Hui, H., Gong, L., Lu, Y., Xue, Z., Liao, H., Chen, F., & Yang, F. (2020). The role of imaging in the detection and management of COVID-19: a review. IEEE reviews in biomedical engineering, 14, 16-29.

Dean, J. C., & Ilvento, C. C. (2006). Improved cancer detection using computer-aided detection with diagnostic and screening mammography: prospective study of 104 cancers. American Journal of Roentgenology, 187(1), 20–28.

Do, C., & Vu, L. (2020). Applications of Digital Image Processing XLIII. International Society for Optics and Photonics, 1151034.

Doi, K. (2007). Computer-aided diagnosis in medical imaging: historical review, current status and future potential. Computerized Medical Imaging and Graphics, 31(4–5), 198–211.

Filip, R., Gheorghita Puscaselu, R., Anchidin-Norocel, L., Dimian, M., & Savage, W. K. (2022). Global challenges to public health care systems during the COVID-19 pandemic: a review of pandemic measures and problems. Journal of Personalized Medicine, 12(8), 1295.

Hafeez, U., Umer, M., Hameed, A., Mustafa, H., Sohaib, A., Nappi, M., & Madni, H. A. (2023). A CNN based coronavirus disease prediction system for chest X-rays. Journal of Ambient Intelligence and Humanized Computing, 14(10), 13179-13193.

Hall, L. O., Paul, R., Goldgof, D. B., & Goldgof, G. M. (2020). Finding covid-19 from chest x-rays using deep learning on a small dataset. arXiv preprint arXiv:2004.02060.

Huang, S., Yang, J., Fong, S., & Zhao, Q. (2021). Artificial intelligence in the diagnosis of COVID-19: challenges and perspectives. International journal of biological sciences, 17(6), 1581.

Gaur, P., Malaviya, V., Gupta, A., Bhatia, G., Pachori, R. B., & Sharma, D. (2022). COVID-19 disease identification from chest CT images using empirical wavelet transformation and transfer learning. Biomedical Signal Processing and Control, 71, 103076.

Harapan, H., Itoh, N., Yufika, A., Winardi, W., Keam, S., Te, H., Megawati, D., Hayati, Z., Wagner, A. L., & Mudatsir, M. (2020). Coronavirus disease 2019 (COVID-19): A literature review. Journal of Infection and Public Health, 13(5), 667–673.

He, X., Wang, S., Shi, S., Chu, X., Tang, J., Liu, X., Yan, C., Zhang, J., & Ding, G. (2020). Benchmarking deep learning models and automated model design for COVID-19 detection with chest CT scans. MedRxiv, 2020–2026.

Heidari, M., Mirniaharikandehei, S., Khuzani, A. Z., Danala, G., Qiu, Y., & Zheng, B. (2020). Improving the performance of CNN to predict the likelihood of COVID-19 using chest X-ray images with preprocessing algorithms. International Journal of Medical Informatics, 144, 104284.

Hussain, Z., Gimenez, F., Yi, D., & Rubin, D. (2017). Differential data augmentation techniques for medical imaging classification tasks. AMIA Annual Symposium Proceedings, 2017, 979.

Jain, R., Gupta, M., Taneja, S., & Hemanth, D. J. (2021). Deep learning based detection and analysis of COVID-19 on chest X-ray images. Applied Intelligence, 51, 1690–1700.

Imani, M. (2021). Automatic diagnosis of coronavirus (COVID-19) using shape and texture characteristics extracted from X-Ray and CT-Scan images. Biomedical Signal Processing and Control, 68, 102602.

Kanji, J. N., Zelyas, N., MacDonald, C., Pabbaraju, K., Khan, M. N., Prasad, A., Hu, J., Diggle, M., Berenger, B. M., & Tipples, G. (2021). False negative rate of COVID-19 PCR testing: a discordant testing analysis. Virology journal, 18(1), 1-6.

Kumar, A., Singh, D., & Yadav, R. S. (2024). Entropy and improved k-nearest neighbor search based under-sampling (ENU) method to handle class overlap in imbalanced datasets. Concurrency and Computation: Practice and Experience, 36(2), e7894.

Kumar, A., Yadav, R. K., & Saini, D. J. B. (2023). Create and implement a new method for robust video face recognition using convolutional neural network algorithm. e-Prime-Advances in Electrical Engineering, Electronics and Energy, 5, 100241.

Kunduru, V. R., & Narayanam, B. (2023). COVID-19 classification based on a convolutional spiking neural network: A modified exponential IF neuron approach. Measurement: Sensors, 29, 100861.

Kaur, T., & Gandhi, T. K. (2022). Classifier fusion for detection of COVID-19 from CT scans. Circuits, Systems, and Signal Processing, 41(6), 3397–3414.

Khattab, R., Abdelmaksoud, I. R., & Abdelrazek, S. (2023). Deep Convolutional Neural Networks for Detecting COVID-19 Using Medical Images: A Survey. New Generation Computing, 41(2), 343–400.

Kinga, D., & Adam, J. B. (2015). A method for stochastic optimization. International Conference on Learning Representations (ICLR), 5, 6.

Kong, W., & Agarwal, P. P. (2020). Chest imaging appearance of COVID-19 infection. Radiology: Cardiothoracic Imaging, 2(1), e200028.

Krizhevsky, A., Sutskever, I., & Hinton, G. E. (2017). ImageNet classification with deep convolutional neural networks. Communications of the ACM, 60(6), 84–90.

Le, J. (2018). Convolutional Neural Networks: The Biologically Inspired Model. Towards Data Science Https://Towardsdatascience. Com/Con Volutional-Neural-Networks-the-Biologicallyinspired-Model-F2d23a301f71.

Lee, E. Y. P., Ng, M.-Y., & Khong, P.-L. (2020). COVID-19 pneumonia: what has CT taught us? The Lancet Infectious Diseases, 20(4), 384–385.

Li, L., Qin, L., Xu, Z., Yin, Y., Wang, X., Kong, B., Bai, J., Lu, Y., Fang, Z., & Song, Q. (2020). Artificial intelligence distinguishes COVID-19 from community acquired pneumonia on chest CT. Radiology.

Mishra, A. K., Das, S. K., Roy, P., & Bandyopadhyay, S. (2020). Identifying COVID19 from chest CT images: a deep convolutional neural networks based approach. Journal of Healthcare Engineering, 2020.

Mohammed, A., Wang, C., Zhao, M., Ullah, M., Naseem, R., Wang, H., Pedersen, M., & Cheikh, F. A. (2020). Weakly-supervised network for detection of COVID-19 in chest CT scans. Ieee Access, 8, 155987–156000.

Mohbey, K. K., Sharma, S., Kumar, S., & Sharma, M. (2022a). COVID-19 identification and analysis using CT scan images: Deep transfer learning-based approach. In Blockchain Applications for Healthcare Informatics (pp. 447–470). Elsevier.

Mohbey, K. K., Sharma, S., Kumar, S., & Sharma, M. (2022b). COVID-19 identification and analysis using CT scan images: Deep transfer learning-based approach. In Blockchain Applications for Healthcare Informatics (pp. 447–470). Elsevier.

Msemburi, W., Karlinsky, A., Knutson, V., Aleshin-Guendel, S., Chatterji, S., & Wakefield, J. (2023). The WHO estimates of excess mortality associated with the COVID-19 pandemic. Nature, 613(7942), 130-137.

Narin, A., Kaya, C., & Pamuk, Z. (2021). Automatic detection of coronavirus disease (covid-19) using x-ray images and deep convolutional neural networks. Pattern Analysis and Applications, 24, 1207–1220.

Nguyen, D., Kay, F., Tan, J., Yan, Y., Ng, Y. S., Iyengar, P., Peshock, R., & Jiang, S. (2021). Deep learning–based COVID-19 pneumonia classification using chest CT images: model generalizability. Frontiers in Artificial Intelligence, 4, 694875.

Ozturk, T., Talo, M., Yildirim, E. A., Baloglu, U. B., Yildirim, O., & Acharya, U. R. (2020). Automated detection of COVID-19 cases using deep neural networks with X-ray images. Computers in Biology and Medicine, 121, 103792.

Panayides, A. S., Amini, A., Filipovic, N. D., Sharma, A., Tsaftaris, S. A., Young, A., Foran, D., Do, N., Golemati, S., & Kurc, T. (2020). AI in medical imaging informatics: current challenges and future directions. IEEE journal of biomedical and health informatics, 24(7), 1837-1857.

Parkinson, C., Matthams, C., Foley, K., & Spezi, E. (2021). Artificial intelligence in radiation oncology: A review of its current status and potential application for the radiotherapy workforce. Radiography, 27, S63-S68.

Pitale, R., Kale, H., Kshirsagar, S., & Rajput, H. (2021). A schematic review on applications of deep learning and computer vision. 2021 Asian Conference on Innovation in Technology (ASIANCON),

Rasheed, J., Hameed, A. A., Djeddi, C., Jamil, A., & Al-Turjman, F. (2021). A machine learning-based framework for diagnosis of COVID-19 from chest X-ray images. Interdisciplinary Sciences: Computational Life Sciences, 13, 103-117.

Sejuti, Z. A., & Islam, M. S. (2023). A hybrid CNN–KNN approach for identification of COVID-19 with 5-fold cross validation. Sensors International, 4, 100229.

Shyni, H. M., & Chitra, E. (2022). A comparative study of X-ray and CT images in COVID-19 detection using image processing and deep learning techniques. Computer Methods and Programs in Biomedicine Update, 2, 100054.

Sitaula, C., & Hossain, M. B. (2021). Attention-based VGG-16 model for COVID-19 chest X-ray image classification. Applied Intelligence, 51, 2850-2863.

Soares, F., Villavicencio, A., Fogliatto, F. S., Pitombeira Rigatto, M. H., José Anzanello, M., Idiart, M. A., & Stevenson, M. (2020). A novel specific artificial intelligence-based method to identify COVID-19 cases using simple blood exams. MedRxiv, 2020.2004. 2010.20061036.

Staszewski, P., Jaworski, M., Cao, J., & Rutkowski, L. (2021). A new approach to descriptors generation for image retrieval by analyzing activations of deep neural network layers. IEEE Transactions on neural networks and learning systems, 33(12), 7913-7920.

Sharifonnasabi, F., Jhanjhi, N. Z., John, J., Obeidy, P., Band, S. S., Alinejad-Rokny, H., & Baz, M. (2022). Hybrid HCNN-KNN model enhances age estimation accuracy in orthopantomography. Frontiers in Public Health, 10, 879418.

Shyu, D., Dorroh, J., Holtmeyer, C., Ritter, D., Upendran, A., Kannan, R., Dandachi, D., Rojas-Moreno, C., Whitt, S. P., & Regunath, H. (2020). Laboratory tests for COVID-19: a review of peer-reviewed publications and implications for clinical use. Missouri Medicine, 117(3), 184.

Silva, P., Luz, E., Silva, G., Moreira, G., Silva, R., Lucio, D., & Menotti, D. (2020). COVID-19 detection in CT images with deep learning: A voting-based scheme and cross-datasets analysis. Informatics in Medicine Unlocked, 20, 100427.

Soares, E., Angelov, P., Biaso, S., Froes, M. H., & Abe, D. K. (2020). SARS-CoV-2 CT-scan dataset: A large dataset of real patients CT scans for SARS-CoV-2 identification. MedRxiv, 2020–2024.

Tasnim, S., & Qi, W. (2023). Progress in Object Detection: An In-Depth Analysis of Methods and Use Cases. European Journal of Electrical Engineering and Computer Science, 7(4), 39–45.

Teymouri, M., Mollazadeh, S., Mortazavi, H., Ghale-Noie, Z. N., Keyvani, V., Aghababaei, F., Hamblin, M. R., Abbaszadeh-Goudarzi, G., Pourghadamyari, H., & Hashemian, S. M. R. (2021). Recent advances and challenges of RT-PCR tests for the diagnosis of COVID-19. Pathology-Research and Practice, 221, 153443.

Vinod, D. N., & Prabaharan, S. (2020). Data science and the role of Artificial Intelligence in achieving the fast diagnosis of Covid-19. Chaos, Solitons & Fractals, 140, 110182.

Wang, S., Kang, B., Ma, J., Zeng, X., Xiao, M., Guo, J., Cai, M., Yang, J., Li, Y., & Meng, X. (2021). A deep learning algorithm using CT images to screen for Corona Virus Disease (COVID-19). European Radiology, 31, 6096–6104.

Watzinger, F., Ebner, K., & Lion, T. (2006). Detection and monitoring of virus infections by real-time PCR. Molecular Aspects of Medicine, 27(2–3), 254–298.

Xiao, C., Choi, E., & Sun, J. (2018). Opportunities and challenges in developing deep learning models using electronic health records data: a systematic review. Journal of the American Medical Informatics Association, 25(10), 1419–1428.

Zhang, S., & Li, J. (2021). Knn classification with one-step computation. IEEE Transactions on Knowledge and Data Engineering.

Zouch, W., Sagga, D., Echtioui, A., Khemakhem, R., Ghorbel, M., Mhiri, C., & Hamida, A. Ben. (2022). Detection of COVID-19 from CT and chest X-ray images using deep learning models. Annals of Biomedical Engineering, 50(7), 825–835.